Indian Journal of Biochemistry & Biophysics
Vol. 40, December 2003, pp. 429-438

Effect of side chain length on the aggregation of amphiphilic 5,10,15-tris (1-methylpyridinium-4-yl)-20-[4-(alkoxy) phenyl] 21H, 23H porphyrin tritosylates

S M S Chauhan*, Anil Kumar, K A Srinivas and M K Mishra

Department of Chemistry, University of Delhi, Delhi 110 007, India

Received 31 March 2003; revised 2 September 2003

Self-aggregation of cationic amphiphilic 5, 10, 15-tris-(1-methylpyridinium-4-yl)-20-[4-(alkoxy)phenyl]-21H, 23H porphyrin tritosylates (2a-e) with different alkoxy chain length in aqueous and binary solvent systems has been studied by UV-visible, fluorescence and ^{1}H NMR spectroscopy. Binary solvent, concentration, ionic strength, presence of surfactants, and temperature govern the aggregations of 2a-e. Porphyrins having side chain length more than ten carbon atoms (2c-e) form higher aggregates, such as vesicles by sonication of dimers formed initially, whereas porphyrins with lesser side chain length (2a & b) form lower aggregates only. Further, the size and the formation of vesicles have been confirmed by transmission electron microscopy (TEM) and dye entrapment experiments for 2e.

Key words: Aggregation, binary solvent, amphiphilic porphyrins, vesicles, higher aggregates.

Self-organization of molecular components to stable and structurally well defined aggregates lead to formation of supramolecules[1-4]. Self-aggregation of natural and synthetic porphyrins significantly alters their physico-chemical and photochemical properties in solution and solid state. Self-organization of amphiphilic porphyrins is dominated by hydrogen bonding[5], π-π stacking interactions and other non-covalent interactions[6-10]. Solvents play a critical role in the self-aggregation by non-covalent interactions. The hydrophobic interactions are stronger in polar protic solvents, whereas hydrogen bonds and electrostatic interactions are favoured in non-polar solvents. Self-aggregation of porphyrins is also implicated in the development of molecular devices and newer materials[11-14]. The synthesis of amphiphilic porphyrins and their aggregation properties in organic[15], aqueous[16-21] and binary solvents systems[15,22-26] have been studied to understand the self-aggregation and other biological phenomenon. The formation of micelles and vesicles in aqueous solution from amphiphilic porphyrins[27-29] has also been reported. However, the studies on the effect of different chain lengths on the aggregation of cationic porphyrins in aqueous solution are limited[29,30]. Herein, we report the synthesis and spectroscopic characterization of 5,10,15-tris (1-methylpyridinium-4-yl)-20-[4-(alkoxy) phenyl]-21H, 23H-porphyrin tritosylates (2a-e) and study of their self-aggregation in aqueous and binary solvent systems by ^{1}H NMR, UV-visible, fluorescence spectroscopy, dye incorporation and transmission electron microscopy (TEM).

Materials and Methods

Methyl bromide, *p*-hydroxybenzaldehyde, 1-bromohexane, 1-bromodecane, 1-bromohexadecane, 1-bromooctadecane, potassium carbonate and propionic acid were purchased from SRL India Ltd. Pyrrole and pyridine 4-carboxyldehyde were purchased from Acros, USA. Methyl-*p*-toluene sulphonate, Sepharose 4B and 2,6-dimethylpyridine were purchased from Fluka. *p*-(Alkoxy)benzaldehydes were prepared from *p*-hydroxybenzaldehyde and corresponding alkyl halides as reported in literature[31].

Absorption spectra were recorded by Shimadzu UV-260 spectrophotometer and the absorption maxima were expressed in nanometers. ^{1}H NMR spectra were recorded on Brucker Heaven (300 MHz) spectrophotometer and the chemical shifts were expressed in ppm. Fluorescence spectra were recorded on Perkins-Elmer L550B spectrophotometer.

*Author for correspondence
Email: smschauhan@chemistry.du.ac.in

Abbreviations: cac, critical aggregation concentration; TEM, transmission electron microscopy; SDS, sodium dodecyl sulphate; CTAB, cetyltrimethylammonium bromide; TMPyP, 5,10,15,20-tetra-(N-methylpyridinium-4-yl)porphyrin., GPC, gel permeation chromatography; DMSO-d_6, dimethyl sulphoxide-d_6.

MALDI-TOF-MS was recorded on Kratos PCKompact SEQ IV instrument. Transmission electron microscopy was carried out on JEOL JEM 2000 EX (TEM) electron microscope at accelerating voltage of 80 KV with different optical magnification and diameters of vesicles were expressed in nanometers.

Experimental section

Porphyrins having different side-chain lengths (1a-e) were synthesized by cyclocondensation of corresponding *p*-(alkyloxy)benzaldehyde, 4-pyridine carboxaldehyde and pyrrole in refluxing propionic acid by minor modifications in literature method[23-32]. N-methylation[33] of 1a-e with methyl *p*-toluenesulphonate in toluene and acetonitrile and purification by repeated column chromatography on silica gel (60-120 mesh) gave 2a-e (Scheme 1). The yields and UV-visible, ^{1}H NMR, MALDI-TOF-MS spectroscopic data of compounds 1a-e and 2a-e are given in Tables 1 and 2, respectively.

General method for the preparation of vesicles of 5,10,15-tris-(1-mehtylpyridinium-4-yl)-20-[4-(alkoxy) phenyl]-21H, 23H porphyrin tritosylates (2a-e)

The unilamellar vesicles of porphyrins 2a-e were prepared by sonication method[34,35]. Minimum amount of methanol was added to a test tube containing 5.0×10^{-5} mol of 2a-e and the solvent evaporated under the nitrogen stream to make the thin film of 2a-e. The thin film was dried under vacuum for 3 hr, deionized double distilled water (1 ml) was added and sonicated for 30 min, at ambient temperature to give a transparent red solution. The vesicular solution was left standing for 1 hr to equilibrate and then run down on gel permeation column (Sepharose 4B, 10×1.5 cm) eluted with water. The fractions were collected at appropriate elution volume and absorption spectra were measured at 428 nm and 454 nm.

Results and Discussion

The self-assembly of amphiphilic molecules in aqueous solution form micelle, hexagonal or lamellar supramolecular structures. The hydrophilic and hydrophobic balance in the amphiphilic molecules strongly affects the suprastructures[35]. The hydrophilic-lipophilic balance and critical aggregation concentration (cac) of amphiphilic porphyrins suggest that they can form supramolecular structures, like micelles or vesicles[36]. UV-visible, fluorescence and ^{1}H NMR spectroscopic studies indicate that amphiphilic porphyrins form dimers in aqueous and

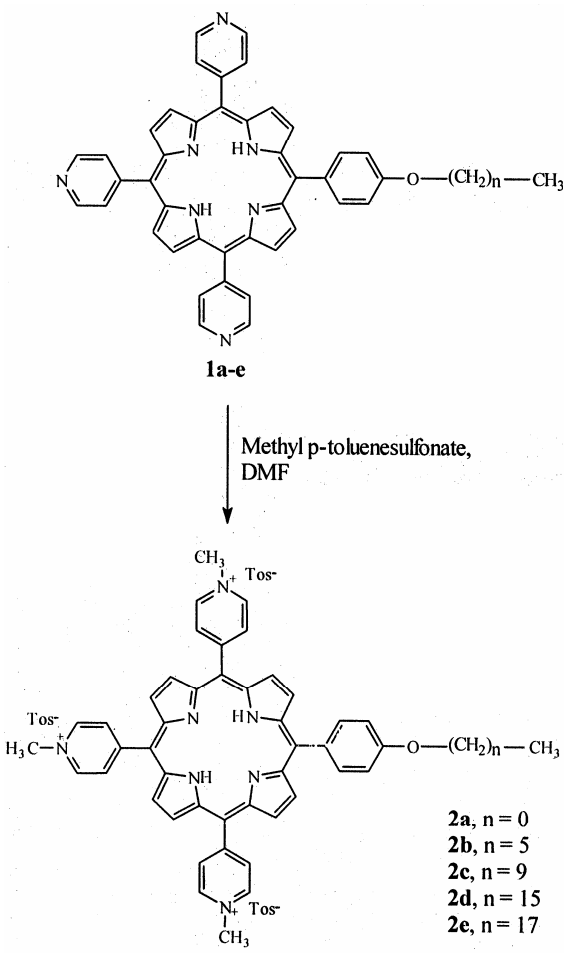

Scheme 1— Synthesis of amphiphilic porphyrinis 2a-e by N-methylation of 1a-e

ethanol-water binary solvent system. Dimerization of porphyrins with longer side chain, such as 2c-e leads to new dimeric amphiphilic structure that further organizes to vesicles. In an earlier study, we observed this type of formation of dimeric amphiphile during the formation of vesicles from amphiphilic 10-alkylisoalloxazines[35].

Absorption spectroscopy

UV-visible spectroscopy is an important and simple technique to understand the self-aggregation of amphiphilic porphyrins in solution[24,25,37,38]. The broadening of Soret peak, change in position and decrease in absorbance intensities of amphiphilic porphyrins have been correlated with aggregate formation[39,40]. The blue shift in Soret band is a sign of H-aggregate formation, whereas the red shift is a sign of J-aggregate formation[29]. UV-visible spectrum of 2a-e in ethanol has a sharp Soret band at 427-428 nm and the apparent changes in Soret maxima absorbance are observed with the increase of water percentage in

Table 1 — Yield and spectral data of compounds 1 **a-e**

Comd.	Yield (%)	^{1}H NMR ($CDCl_3$)/ δ ppm	UV-visible ($CHCl_3$) λ_{max}/nm (Abs.)	MALDI-TOF MASS
1a	12.5	9.05 (d, J=7.8 Hz, 6H, 3,5-py); 8.96 (d, J=7.6 Hz, 2H, β-pyrrolic); 8.85 (s, 4H, β-pyrrolic); 8.81 (d, J=7.6 Hz, 2H, β-pyrrolic); 8.15 (d, J=7.8 Hz, 6H, 2,6-py); 8.11 (dd, J=6.9 Hz & 2.4 Hz, 2H, 2,6-Ph); 7.31 (dd, J=6.9 Hz & 2.4 Hz, 2H, 3,5-Ph); 4.10 (s, 3H, OCH_3); -2.86 (s, 2H, internal NH)	417 (0.977), 518 (0.089), 552 (0.021), 578 (0.017), 646 (0.009)	646.7 (M+1)
1b	13.2	9.00 (d, J=7.7 Hz, 6H, 3,5-py); 8.94 (d, J=7.7 Hz, 2H, β-pyrrolic); 8.83 (s, 4H, β-pyrrolic); 8.79 (d, J=7.7 Hz, 2H, β-pyrrolic); 8.21 (d, J=7.7 Hz, 6H, 2,6-py); 8.15 (dd, J=7.0 Hz & 2.3 Hz, 2H, 2,6-Ph); 7.31 (dd, J=7.0 Hz & 2.3 Hz, 2H, 3,5-Ph); 4.17 (t, J=7.3 Hz, 2H, OCH_2); 1.81 (q, J=7.3 Hz, 2H, OCH_2CH_2); 1.29 (m, 6H, C-chain); 0.89 (t, J=7.2 Hz, 3H, CH_3); -2.85 (s, 2H, internal NH)	417 (1.009), 519 (0.098), 551 (0.024), 569 (0.021), 647 (0.010)	716.8 (M+1)
1c	11.1	9.12 (d, J=7.8 Hz, 6H, 3,5-py); 9.03 (d, J=7.5 Hz, 2H, β-pyrrolic); 8.98 (s, 4H, β-pyrrolic); 8.88 (d, J=7.5 Hz, 2H, β-pyrrolic); 8.36 (d, J=7.8 Hz, 6H, 2,6-py); 8.10 (dd, J=7.1 Hz & 2.3 Hz, 2H, 2,6-Ph); 7.30 (dd, J=7.1 Hz & 2.3 Hz, 2H, 3,5-Ph); 4.25 (t, J=6.8 Hz, 2H, OCH_3); 1.91 (q, J=6.8 Hz, 2H, OCH_2CH_2); 1.29 (m, 16H, C-chain); 0.90 (t, J=6.7 Hz, 3H, CH_3); -2.86 (s, 2H, internal NH)	418 (0.956), 518 (0.087), 551 (0.019), 578 (0.016), 647 (0.008)	773.0 (M+1)
1d	12.3	9.08 (d, J=7.8 Hz, 6H, 3,5-py); 9.02 (d, J=7.6 Hz, 2H, β-pyrrolic); 8.88 (s, 4H, β-pyrrolic); 8.83 (d, J=7.6 Hz, 2H, β-pyrrolic); 8.19 (d, J=7.8 Hz, 6H, 2,6-py); 8.13 (dd, J=7.4 & 2.4 Hz, 2H, 2,6-Ph); 7.33 (dd, J=7.4 & 2.4 Hz, 2H, 3,5-Ph); 4.35 (t, J=6.8 Hz, 2H, OCH_2); 1.95 (q, J=6.8 Hz, 2H, OCH_2CH_2); 1.33 (m, 26H, C-chain); 0.97 (t, J=6.7 Hz, 3H, CH_3); -2.85 (s, 2H, internal NH)	418 (0.987), 519 (0.088), 552 (0.020), 578 (0.017), 647 (0.009)	857.1 (M+1)
1e	12.8	9.11 (d, J=7.8 Hz, 6H, 3,5-py); 9.02 (d, J=7.7 Hz, 2H, β-pyrrolic); 8.94 (s, 4H, β-pyrrolic); 8.87 (d, J=7.7 Hz, 2H, β-pyrrolic); 8.21 (d, J=7.8 Hz, 6H, 2,6-py); 8.13 (dd, J=7.3 & 2.27 Hz, 2H, 2,6-Ph); 7.30 (dd, J=7.3 & 2.2 Hz, 2H, 3,5-Ph); 4.39 (t, J=6.8 Hz, 2H, OCH_2); 1.89 (q, J=6.8 Hz, 2H, OCH_2CH_2); 1.34 (m, 30H, C-chain); 0.92 (t, J=6.7 Hz, 3H, CH_3); -2.87 (s, 2H, internal NH)	418 (1.005), 518 (0.089), 552 (0.021), 578 (0.018), 647 (0.010)	885.2 (M+1)

Table 2 — Yield and spectral data of amphiphilic porphyrins 2 **a-e**

Compd.	Yield (%)	^{1}H NMR (DMSO-d_6)/ δ ppm	UV-visible (ethanol) λ_{max}/nm (Abs.)	Fluorescence (Ethanol) λ_{max}/nm (Abs.)	MALDI-TOF MASS
2a	87.7	9.52 (d, J=7.7 Hz, 6H, 3,5-py); 8.95 (m, 8H, β-pyrrolic); 8.70 (d, J=7.7 Hz, 6H, 2,6-py); 7.97 (d, J=7.2 Hz, 2H, 2,6-Ph); 7.69 (d, J=6.9 Hz, 6H, tosylate); 7.30 (d, J=7.2 Hz, 2H, 3,5-Ph); 7.04 (d, J=7.9 Hz, 6H, tosylate); 4.82 (s, 9H, NCH_3); 4.11 (s, 3H, OCH_3); 2.2 (s, 9H, CH_3 tosylate); -2.67 (s, 2H, internal NH)	427 (5.012), 521 (3.876), 553 (3.670), 587 (3.472), 646 (3.254)	653 (23.5), 719 (8.3) 653 (10.2), 718 (4.3)[a]	1205.4 (M+1)
2b	89.3	9.55 (d, J=7.7 Hz, 6H, 3,5-py); 8.96 (m, 8H, β-pyrrolic); 8.67 (d, J=7.7 Hz, 6H, 2,6-py); 8.02 (d, J=7.3 Hz, 2H, 2,6-Ph); 7.71 (d, J=6.9 Hz, 6H, tosylate); 7.34 (d, J=7.3 Hz, 2H, 3,5-Ph); 7.01 (d, J=6.9 Hz, 6H, tosylate); 4.78 (s, 9H, NCH_3); 4.15 (s, 2H, OCH_2); 2.26 (s, 9H, CH_3 tosylate); 1.92 (q, J=6.7 Hz, 2H, OCH_2CH_2); 1.19 (m, 6H, C-chain); 0.89 (t, J=6.6 Hz, 3H, CH_3); -2.69 (s, 2H, internal NH)	427 (5.019), 521 (3.776), 552 (3.647), 587 (3.437), 646 (3.249)	653 (22.8), 719 (8.1) 652 (8.6), 718 (4.1)[a]	1275.5 (M+1)
2c	84.8	9.53 (d, J=7.7 Hz, 6H, 3,5-py); 9.02 (m, 8H, β-pyrrolic); 8.86 (d, J=7.7 Hz, 6H, 2,6-py); 8.08 (d, J=7.3 Hz, 2H, 2,6-Ph); 7.67 (d, J=6.9 Hz, 6H, tosylate); 7.36 (d, J=7.3 Hz, 2H, 3,5-Ph); 7.02 (d, J=6.9 Hz, 6H, tosylate); 4.76 (s, 9H, NCH_3); 4.28 (t, J=6.8 Hz, 2H, OCH_2); 2.25 (s, 9H, CH_3 tosylate); 1.98 (q, J=6.8 Hz, 2H, OCH_2CH_2); 1.26 (m, 16H, C-chain); 0.91 (t, J=6.8 Hz, 3H, CH_3); -2.73 (s, 2H, internal NH)	428 (5.212), 522 (3.987), 553 (3.767), 587 (3.547), 648 (3.325)	654 (22.3), 718 (8.4) 652 (2.3), 717 (1.2)[a]	1331.64 (M+1)
2d	87.1	9.52 (d, J=7.8 Hz, 6H, 3,5-py); 9.00 (m, 8H, β-pyrrolic); 8.81 (J=7.8 Hz, 6H, 2,6-py); 7.97 (d, J=7.2 Hz, 2H, 2,6-Ph); 7.65 (d, J=6.8 Hz, 6H, tosylate); 7.28 (d, J=7.2 Hz, 2H, 3,5-ph); 7.08 (d, J=6.8 Hz, 6H, tosylate); 4.77 (s, 9H, NCH_3); 4.24 (t, J=6.8 Hz, 2H, OCH_2); 2.18 (s, 9H, CH_3 tosylate); 1.87 (q, J=6.8 Hz, 2H, OCH_2CH_2); 1.26 (m, 26H, C-chain); 0.79 (t, J=6.8 Hz, 3H, CH_3); -2.78 (s, 2H, internal NH)	427 (5.010), 521 (3.872), 553 (3.667), 587 (3.474), 647 (3.245)	654 (21.4), 719 (7.7) 652 (1.2), 718 (0.6)[a]	1415.8 (M+1)
2e	88.4	9.48 (d, J=7.7 Hz, 6H, 3,5-py); 8.87 (m, 8H, β-pyrrolic); 8.78 (d, J=7.7 Hz, 6H, 2,6-py); 7.86 (d, J=7.3 Hz, 2H, 2,6-Ph); 7.63 (d, J=6.8 Hz, 6H, tosylate); 7.27 (d, J=7.3 Hz, 2H, 3,5-Ph); 6.96 (d, J=6.7 Hz, 6H, tosylate); 4.74 (s, 9H, NCH_3); 4.07 (t, J=6.7 Hz, 2H, OCH_2); 2.14 (s, 9H, CH_3 tosylate); 1.79 (q, J=6.4 Hz, 2H, OCH_2CH_2); 1.18 (m, 30H, C-chain); 0.78 (t, J=6.4 Hz, 3H, CH_3); -2.76 (s, 2H, internal NH)	428 (5.101), 522 (3.871), 553 (3.665), 588 (3.467), 647 (3.243)	654 (19.8), 719 (6.8) 653 (0.8), 718 (0.2)[a]	1443.85 (M+1)

[a]Fluorescence values in the presence of NaCl (0.05 *M*) in aqueous solution.

ethanol-water binary solvent systems (Fig. 1A). The blue shift of Soret peak (4-5 nm) in aqueous (100%) solution of 2a-e indicates the existence of dimers or higher aggregates of H-type. Earlier, this type of blue shift in Soret peak was observed in the dimerization or trimerization of porphyrins in aqueous solution[41,42].

The half-width ($W_{1/2}$) of Soret peaks is correlated to the degree of aggregation of amphiphilic porphyrins[22,25]. The increase in $W_{1/2}$ of Soret peak of 2a-e in ethanol-water binary solvent systems has been observed with increase in water percentage (Fig. 2). The $W_{1/2}$ is 28 nm in ethanol and it increases from 36 nm to 48 nm in water with increase in carbon chain in alkoxy group at C-4′ position of porphyrins 2a-e. The change in $W_{1/2}$ is in good agreement with the formation of aggregates in aqueous solution and ethanol water binary solvent systems[22,23,25].

The critical aggregation concentration (cac) is typically obtained by monitoring a specific physical property of the solution as a function of concentration of monomeric species. The Lambert-Beer's law states that absorbance is directly proportional to concentration and deviation from linearity in the graph of *vs.* absorbance (Fig. 3) may be assigned as cac of porphyrins 2a-e. The absorbance of Soret band of 2e increases with the increase in concentration up to 1.0×10^{-5} *M* in aqueous solution and the deviation begins to appear at a concentration of about 1.5×10^{-5} *M* and this value may be assigned as cac for 2e. At concentration higher than 3.0×10^{-5} *M*, the Soret band

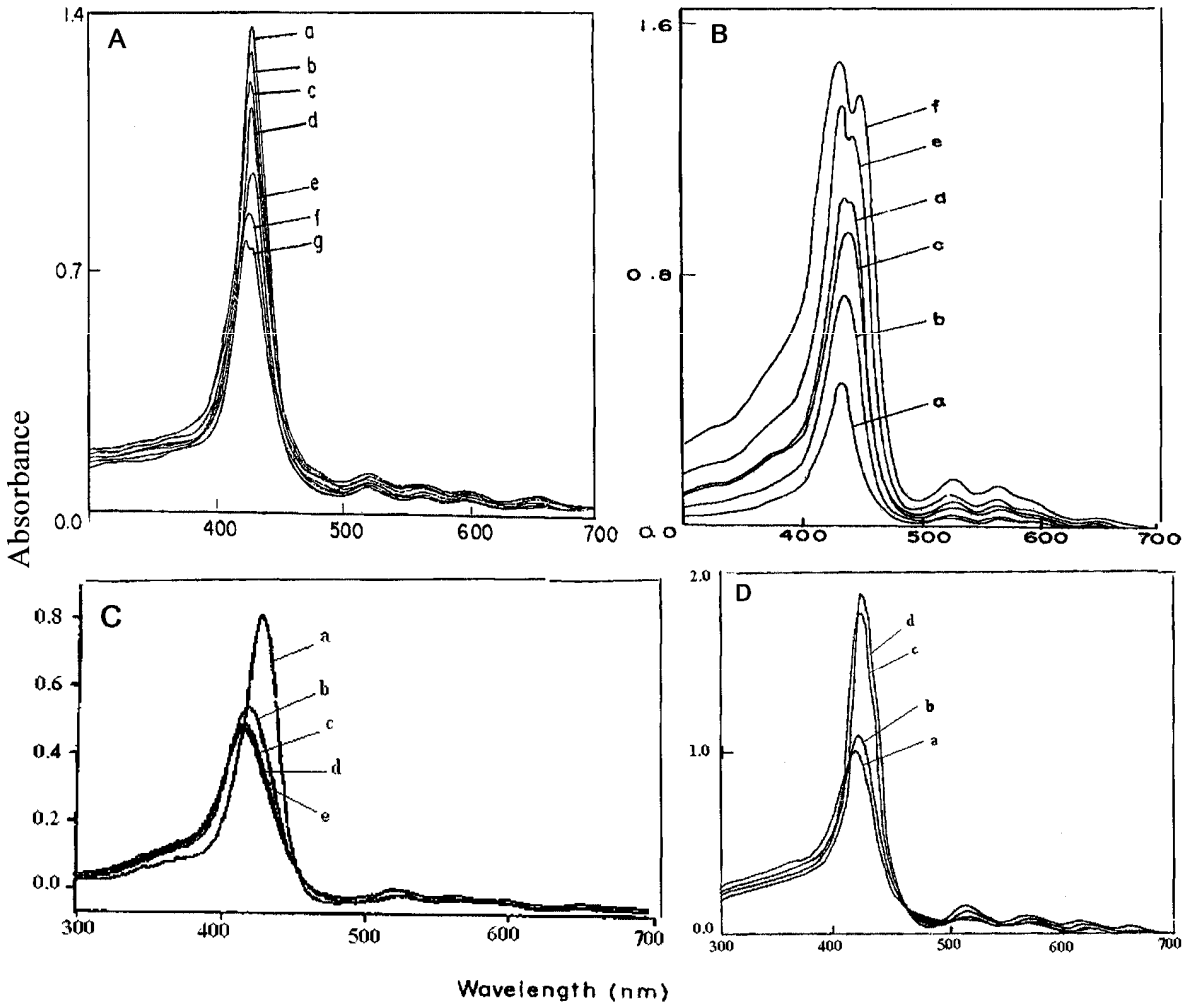

Fig. 1—UV-visible spectra of amphiphilic porphyrin 2e: (**A**) in ethanol:water binary solvent system, where [2e]=2.0×10^{-5} *M*; a, ethanol (100%); b, ethanol:water (50:50); c, ethanol:water (40:60); d, ethanol:water (30:70); e, ethanol:water (20:80); f, ethanol:water (10:90); and g, water (100%); (**B**) at different concentration [a, 5.0×10^{-6}; b, 2.0×10^{-5} ; c, 3.0×10^{-5}; d, 4.0×10^{-5}; e, 5.0×10^{-5}; and f, 1.0×10^{-4}; (**C**) under different NaCl concentrations: a, 0.0 *M*; b, 0.01 *M*; c, 0.05 *M*; d, 0.10 *M*; e, 0.50 *M*, where [2e]=2.0×10^{-5} *M*; (**D**) in different surfactant solutions: a, water; b, CTAB; c, Triton X-100; and d, SDS, where [2e]= 2.0×10^{-5} *M*.

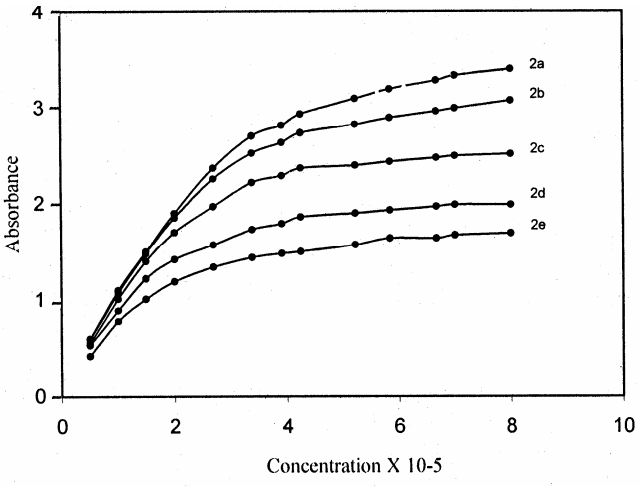

Fig. 3—Graph for concentration *vs* absorbance of Soret peak of porphyrins 2a-e in water

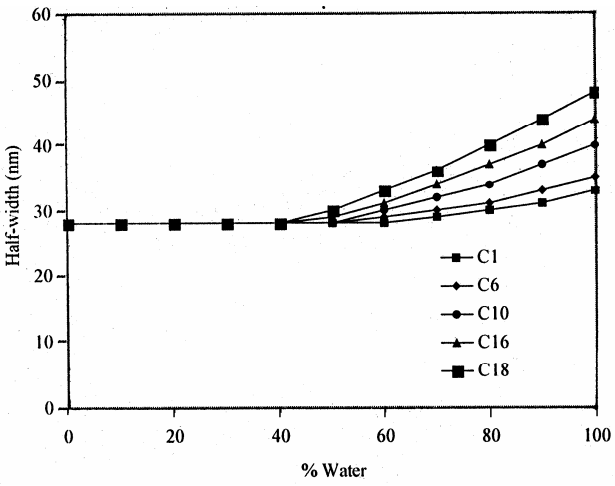

Fig. 2—Half-width (W1/2) of Soret peak of amphiphilic porphyrins 2a-e in ethanol: water binary solvent system

of 2e splits in two bands, one with lower intensity at 417 nm and other with higher intensity at 436 nm (Fig. 1B). The splitting of Soret of 2e at higher concentration may be attributed to the formation of higher aggregates, such as micelles or vesicles from the amphiphilic porphyrins in aqueous solution[24,43,44]. Similar type of Soret splitting is observed in porphyrins 2c and 2d, whereas splitting of Soret is less prominent in porphyrins 2a and 2b, but Soret band becomes broad.

The presence of salts, such as KNO_3 and NaCl facilitates the self-aggregation of water-soluble cationic porphyrins[45,46]. Addition of 0.01 mole/L NaCl solution to an aqueous solution of 2e (2.0×10^{-5} *M*) results in blue shift of Soret to 419 nm from 422 nm with decrease in the absorbance of Soret peak. As the concentration of salt is increased to 0.50 mole/L, Soret of 2e is further blue shifted to 417 nm (Fig. 1C). These results show that the increase of ionic strength increases the self-aggregation of 2e. Similar behaviour is observed with porphyrins 2c and 2d, but there is no much change in the Soret or absorbance in the case of 2a and 2b. The difference in the effect of salt on absorption spectra of 2a-e indicates that porphyrins with small side chain length do not form higher aggregates in water, even on increasing ionic strength.

The presence of surfactants is reported to dissociate the aggregates of ferroheme-pyridine complexes, protoporphyrin-IX and synthetic amphiphilic porphyrins into monomer[17,25,47,48]. As the SDS (an anionic surfactant) is added to aqueous solution of 2e (2.0×10^{-4} *M*), the absorption spectrum changes drastically. The sharp Soret peak with increase in absorbance intensity and a red shift from 422 nm to 428 nm has been observed (Fig. 1D). Further, half-width ($W_{1/2}$) is also decreased from 48 nm to 28 nm, on addition of SDS to aqueous solution of 2e. The change in absorption spectrum in the presence of SDS corresponds with the monomeric porphyrin 2e suggests that the aggregated porphyrin 2e is dissociated into monomer in the presence of SDS. The presence of neutral surfactant Triton X-100 (a co-polymer of ethylene oxide and octyl phenol) also shows similar results, but the changes are less, compared to SDS. However, the presence of cationic surfactant (CTAB) did not show any effect on the Soret of 2e (Fig. 1D). This is in agreement with the earlier reports that cationic porphyrins are monomerized in the presence of anionic micelles[16], whereas anionic porphyrins are monomerized in the cationic micelle solutions[49]. Similar behaviour is observed, when SDS or Triton X-100 solution is added to 2d and 2c, but the changes in absorption spectra are less pronounced in case of 2a and 2b. Thus, porphyrins 2c-e mainly exist as higher aggregate in aqueous solution, whereas 2a and 2b in dimeric form and they are all found to dissociate to monomer in the presence of surfactants.

Fluorescence study

The well-resolved fluorescence peaks at 653-654 nm and 717-719 nm in ethanol are observed for porphyrins 2a-e (Table 2). The intensity of fluorescence peaks is gradually decreased as the

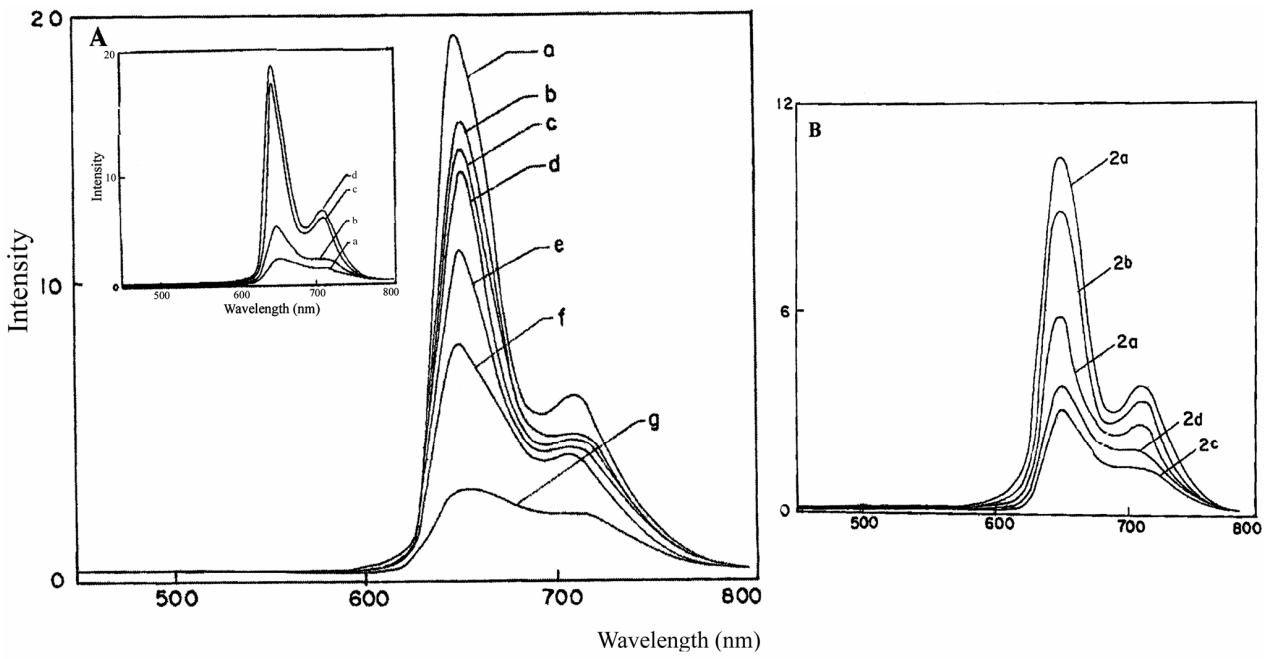

Fig. 4—Fluorescence spectra of (**A**) porphyrin 2e in ethanol:water binary solvent system, where [2e]= 2.0×10^{-5} *M*; a, ethanol (100%); b, ethanol:water (50:50); c, ethanol:water (40:60); d, ethanol:water (30: 70); e, ethanol:water (20:80); f, ethanol:water (10: 90); and g, water (100%). **Inset**: Fluorescence spectra of 2e in different surfactant solutions: a, water; b, CTAB; c, Triton X-100; and d, SDS; (**B**) of porphyrins 2a-e (2.0×10^{-5} *M*) in water.

percentage of water is increased in the ethanol-water binary solvent system. The fluorescence spectrum of porphyrin 2e with different percentage of water in ethanol (Fig. 4A) indicates that it mainly exists as monomer in ethanol solution, whereas as dimer or higher aggregate in aqueous solution. Earlier, decrease in the intensity of fluorescence peaks has been reported in dimer formation[16,17] of TMPyP at room temperature. Further, the decrease in intensity of fluorescence peaks is more prominent in the case of 2e, compared to 2a in aqueous solution (Fig. 4B). The effect of concentration on the fluorescence spectra of 2a-e is studied by changing concentration from 5.0×10^{-6} *M* to 1.0×10^{-4} *M*. A significant decrease in the intensities of fluorescence peaks of 2c-e is observed with increase of concentration above their cac value, compared to 2a and 2b. The quenching of fluorescence by increasing concentration may be attributed to the formation of face-to-face self-aggregates of amphiphilic porphyrins. Addition of NaCl solution to 2a-e also decreased the intensities of fluorescence peaks, suggesting that the increase of ionic strength enhances the aggregate formation. The change in intensities of fluorescence peaks with addition of NaCl solution is less in the case 2a and 2b, compared to 2c-e. Addition of surfactants (SDS or Triton X-100) to aqueous solution of porphyrins 2a-e increased the intensities of fluorescence peaks and resolved them into two peaks, showing that the aggregates are monomerized in the presence of surfactants. The effect of different surfactants on the fluorescence spectra of 2e is shown in an inset in Fig. 4A. The increase in intensities of the fluorescence peaks is negligible for 2a and 2b, as compared to 2c-e. However, similar to absorption spectral changes, the addition of cationic surfactants (CTAB) to porphyrins 2a-e results no change in intensities, suggesting that they exist as aggregates in CTAB solution.

Proton nuclear magnetic resonance (^{1}H NMR) study

The ^{1}H NMR spectra have been used to determine the monomeric and dimeric forms of cationic porphyrins in organic and aqueous solutions[17,25,43,]. The effect of alkoxy chain length on the self-aggregation of porphyrins 2a-e is studied, using ^{1}H NMR spectroscopy. The sharp peaks at 9.02-8.87 ppm for β-pyrrolic protons in DMSO-d_6 indicate that porphyrins 2a-e are in monomeric form. The peaks for β-pyrrolic protons of 2c-e have broadened in D_2O than the signals in DMSO-d_6 due to self-aggregation in D_2O, but this broadening is very less in the case of

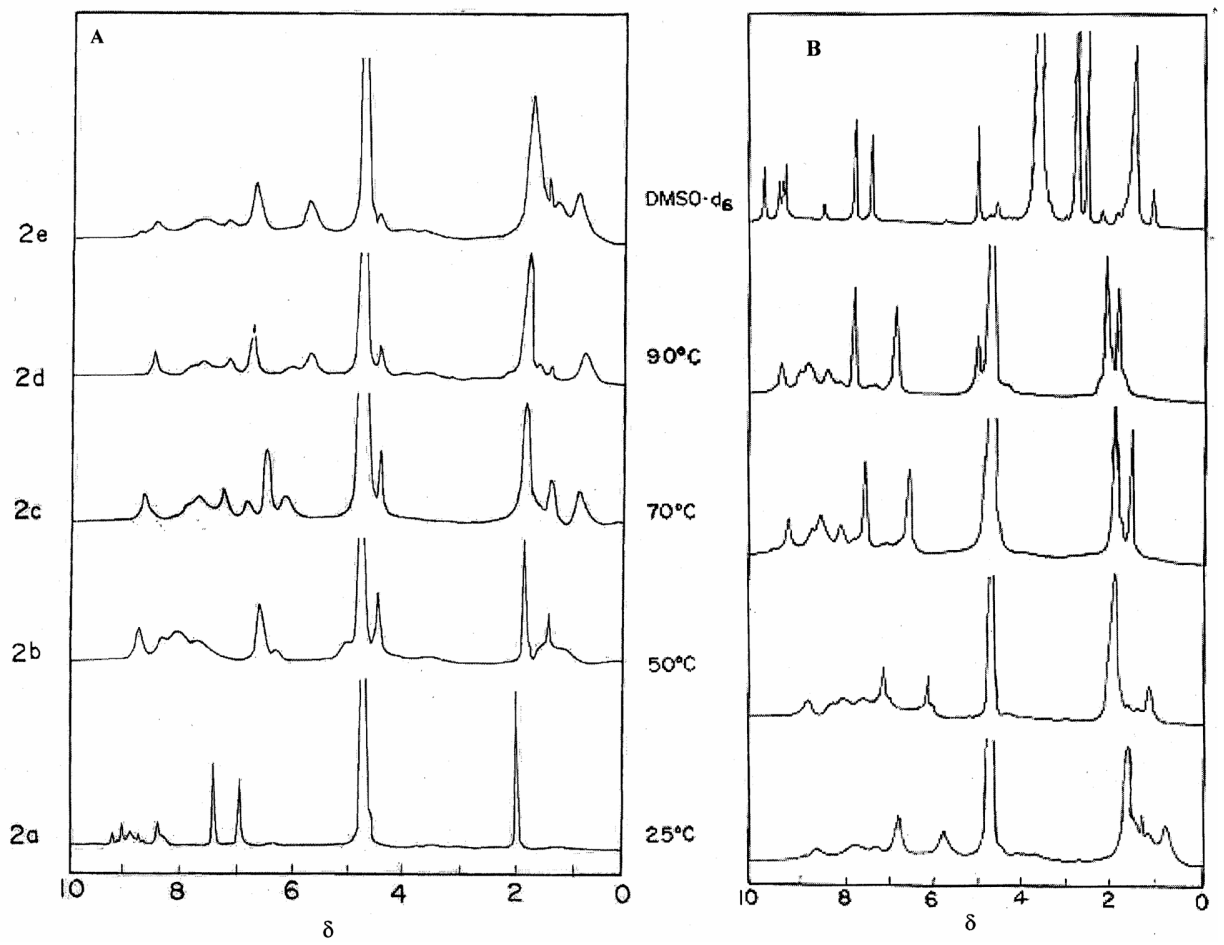

Fig. 5—[1]HNMR spectra of (**A**) porphyrins 2a-e (5.0×10^{-5} *M*) in D_2O at 25°C (**B**) porphyrin 2e (5.0×10^{-5} *M*) in D_2O at different temperatures

2a and 2b. The ^{1}H NMR spectra of porphyrins 2a-e in D_2O at 5.0×10^{-3} *M* concentration are shown in Fig. 5A. It is interesting to note that the each signal of porphyrin 2e has shifted to lower magnetic fields, compared to 2a. The shift in signals of porphyrins 2b-d is intermediate to the extremes and this is in agreement with UV-visible and fluorescence spectral data that higher aggregates or vesicle formation increases with the increase of alkoxy side chain length. The changes in the chemical shifts can be explained by the formation of partially side slipped face-to-face self-aggregates, where ring current of porphyrin ring will affect the proton shift. Self-aggregation of porphyrin 2e (5.0×10^{-3} *M*) is also studied from ^{1}H NMR spectral changes as a function of temperature. At 25°C, all proton signals are broad in D_2O, indicating the formation of self-aggregate and they converted to sharp signals at 90°C (Fig. 5B). Further, three types of β-pyrrolic protons of 2e are clearly distinguished and all the proton signals are shifted to higher magnetic field at higher temperatures, showing that the higher aggregate at room temperature has dissociated to monomer at high temperature. The dissociation may be due to the fast tautomerization of inner N-D deuterons at high temperature. Thus, the difference in ^{1}H NMR spectra of porphyrins 2a-e can be interpreted as there is difference in the degree of aggregation of these porphyrins and this is because of difference in their alkoxy side chain length

Characterization of vesicle formation in aqueous solution

Small unilamellar vesicles are prepared by the ultrasonication of the thin film of amphiphilic porphyrins as described in 'Experimental Section'. The different fractions from gel permeation column on Sepharose 4B are collected at appropriate elution

volume and analyzed by absorbance spectroscopy. The splitted Soret at 417 nm and 454 nm is observed for fractions (5^{th}-9^{th}) in UV-visible spectra (Fig. 6), but there is no prominent Soret splitting and the absorbance of lower wavelength is increasing after 9^{th} fraction. The presence of splitted Soret in 5^{th} to 9^{th} fraction after GPC shows that the highly aggregated porphyrin molecules (i.e. vesicles) have eluted first. The absence of splitted Soret in the subsequent fractions indicates that they are having lower aggregates only. Similarly, the decrease in the intensity of fluorescence peaks of these fractions (5^{th} -9^{th}) also confirmed the presence of higher aggregates. It is interesting to note that after sonication and GPC, the intensities of fluorescence peaks are much lower than the intensities of 2e before sonication indicating that sonication resulted in more ordered structures of porphyrin 2e.

The formation of vesicles or higher aggregates can also be confirmed from the effect of surfactants on the Soret band. Addition of SDS solution to 5^{th} fraction of GPC results in disappearance of splitted Soret and give a new sharp peak at 427 nm, which is similar when surfactant is added to aqueous solution of 2e before sonication. The red shift and splitting in Soret peak is due to the presence of J-aggregates at higher concentrations, whereas broadening of Soret peak with blue shift is because of the presence of H-aggregate. Further, the growing H-aggregates may assemble into J-aggregates as more rigid structures after reorganization of their overall structure. This is similar to the transition of H to J-aggregates, upon increasing the concentration[27]. Furthermore, the

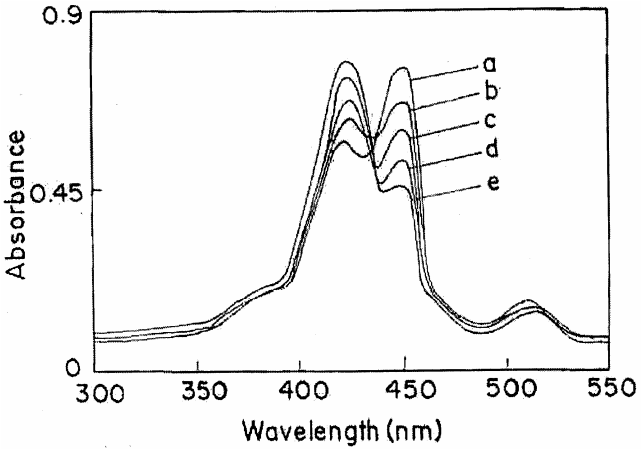

Fig. 6—UV-visible spectra of different gel permeation chromatography fractions of porphyrin 2e (2×10^{-5} *M*) after sonication

electrostatic repulsion between porphyrinic planes may favour face-to-face aggregates, rather than edge-to-edge aggregates. Earlier, of slipped face-to-face J-aggregates formation at higher concentration was observed with TriMPyP[28].

Similar results have been obtained with 2c and 2d, but porphyrins 2a and 2b behave differently. No such Soret splitting is observed in the case of 2a and 2b, even after sonication and GPC. The above results indicate that porphyrins with small alkoxy side chain lengths form premicellar or other unorganized aggregates only and the vesicles (higher aggregates). Porphyrins with longer chain length form organized structures on sonication of their aqueous solution above their cac value.

(b) Transmission electron microscopy (TEM)

TEM has been used to measure the size and study the organized structure formation, like micelles[12,25] or vesicles[26] by self-aggregation of amphiphilic porphyrins. Electron micrographs of porphyrins 2a-e are shown in Fig. 7. As seen from electron micrograph, the diameter of spherical unilamellar vesicles of porphyrins 2c-e varies between 250 to 285 nm. Aqueous dispersion of vesicles was stable for several weeks. Electron micrographs also clearly show that porphyrins 2a and 2b could not form spherical unilamellar vesicles, but they exist as premicellar or other unorganized aggregates.

(c) Dye entrapment experiment

The entrapment of dye in aqueous core of vesicle is responsible for the formation of closed vesicles from surfactants. The water-soluble dye (phthalocyanine) entrapped vesicles from porphyrins are prepared by co-sonication method[35]. The entrapment of dye is confirmed by gel permeation chromatography (Sepharose 4B column, 10×1.5 cm) and monitored by the absorption spectroscopy at 706 nm and 454 nm based on water-soluble phthlocyanine and porphyrin (2e), respectively. The elution profile shows that porphyrin (2e) and phthlocyanine elute at the same elution volume (Fig. 8). The coincidence of curves with each other indicates that phthlocyanine is entrapped in the vesicles formed by porphyrin 2e. When similar experiments are carried out with porphyrins containing small side chain lengths, the dye is not co-eluted with porphyrin fractions indicating that the dye could not be entrapped as porphyrins 2a and 2b are not forming vesicles. Thus,

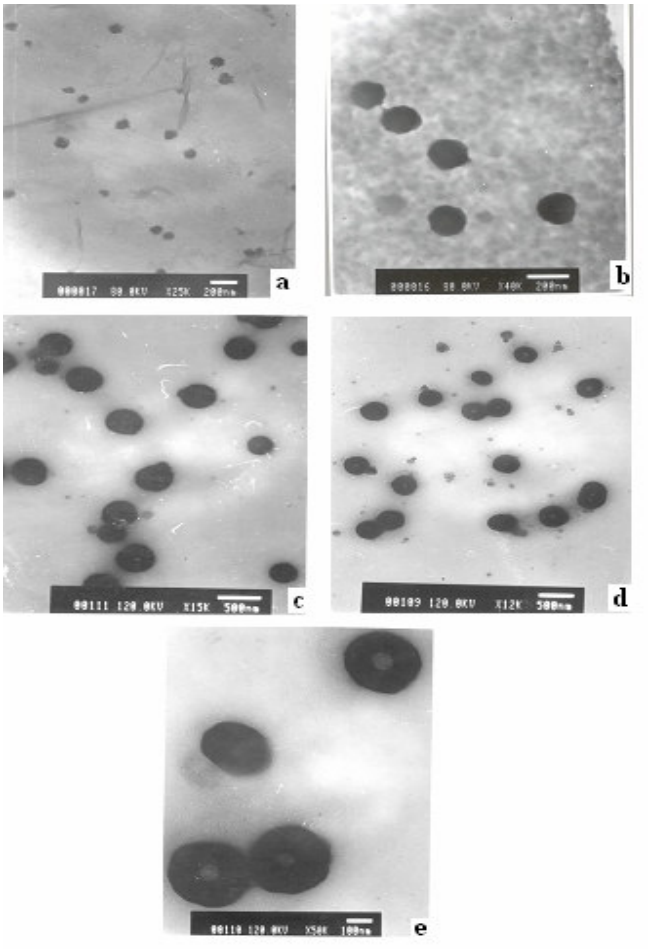

Fig. 7—Transmission electron micrograph of amphiphilic porphyrins [a, 2b; b, 2c; c, 2d; d, 2e; and e, enlarged view of 2e]

the dye entrapment experiments also support the formation of closed vesicles of porphyrins containing alkoxy side chain of ten or more carbon atoms.

Conclusion

Cationic amphiphilic porphyrins, 5, 10, 15-tris-(1-methylpyridinium-4-yl)-20-[4-(alkoxy)phenyl]-21H, 23H porphyrin tritosylates (2a-e) with different alkoxy chain length are synthesized and their aggregation is studied. The chain length of alkoxy side chain governs their aggregations in aqueous and ethanol:water binary solutions. They form dimers in aqueous and ethanol:water binary solvent system, as indicated by UV-visible, fluorescence and ^{1}H NMR spectroscopic studies. Dimerization of longer side chain porphyrins, such as 2c-e leads to new dimeric amphiphilic structure that further organizes to vesicles. Porphyrins with short carbon chain length (2a & 2b) remain as premicellar or other unorganized aggregates. The appropriate hydrophobicity is

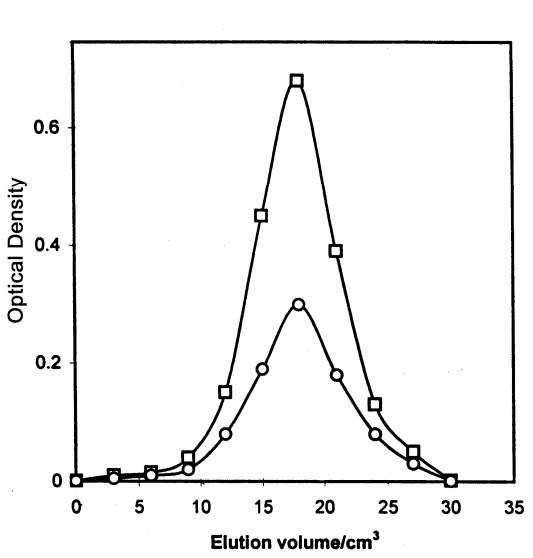

Fig. 8—Elution profile of dye entrapped vesicles obtained from amphiphilic prophyrin 2e on Sepharose 4B column [Elution with water monitored at 454 nm (□) and 706 nm (o) for porphyrin 2e and water soluble phthalocynime dye, respectively]

necessary for the formation of higher aggregates (vesicles) on sonication. The extended J-aggregation depends on concentration, temperature and ionic strength of aqueous solution of porphyrins.

Acknowledgement

We are grateful for financial assistance to the Council of Scientific and Industrial Research (CSIR), New Delhi, India. One of the authors (AK) is thankful to University Grant Commission (UGC), New Delhi, for grant of Senior Research Fellowship.

References

1 Conn M M & Rebek Jr J (1997) *Chem Rev* 97, 1647-1668
2 Terfort A, Bowden N & Whiteside G M (1997) *Nature (London)* 386, 162-164
3 Whiteside G M, Simanek E E, Mathias J P, Chin C T, Mannen M & Gordon G M (1995) *Acc Chem Res* 28, 37-44
4 Philip D & Stoddart J F (1996) *Angew Chem Int Ed Engl* 35, 1154-1596
5 Ariga K & Kunitake T (1998) *Acc Chem Res* 31, 371-378
6 Jin R, Aoki S & Shima K (1997) *J Chem Soc Faraday Trans* 93, 3945-3953
7 Hunter C A & Sanders J K M (1990) *J Am Chem Soc* 112, 5525-5534
8 Hunter C A (1994) *Chem Soc Rev* 23, 101-109
9 Sato T, Ogawa T & Kano K (1984) *J Phys Chem* 88, 3678-3782
10 Hayashi T & Ogashi H (1997) *Chem Soc Rev* 26, 355-364
11 Desiraju G R (1995) *Angew Chem Int Ed Engl* 34, 2311-2327
12 Fuhrhop J H, Demoulin C, Boettchar C, Koning J & Siggel U (1992) *J Am Chem Soc* 114, 4159-4165

13 Tsuchida E, Komatsu T, Toyano N, Komamoto S I & Nishide N (1993) *J Chem Soc Chem Commun* 1731-1733
14 Tsuchida E, Komatsu T, Arai K & Nishide H (1993) *J Chem Soc Chem Commun* 730-732
15 Yamamura T (1977) *Chem Lett* 773-775
16 Kano K, Miyake T, Uomoto K, Sato T, Ogawa T & Hashimoto S (1983) *Chem Lett* 1867-1872
17 Kano K, Nakajima T, Takei T & Hashimoto S (1987) *Bull Chem Soc Jpn* 60, 1281-1287
18 Pasternack R F, Gibbs E J, Gaudemer A, Antebi A, Bassner S, Poy L D, Turner D H, Williams A, Laplace F, Lansard M H, Merienne C & Perree-Fauvet M (1985) *J Am Chem Soc* 107, 8179-8186
19 Chandrashekar T K, Van Willigen H & Ebserole M H (1984) *J Phys Chem* 88, 4326-433
20 Fuhrhop J H & Baccouche M (1976) *Liebigs Ann Chem* 2058-2064
21 Leighten P, Cowan J A, Abraham R J & Sander J K M (1988) *J Org Chem* 53, 733-740
22 Sharma T K & Chauhan S M S (1995) *Ind J Heterocycl Chem* 4, 173-178
23 Chauhan S M S, Sharma T K & Mishra M K (1996) *Ind J Heterocycl Chem* 6, 15-20
24 Tajima K, Ishikawa Y, Mukai K, Ishizu K & Sakarai H (1984) *Bull Chem Soc Jpn* 57, 3587-3588
25 Guilard R, Senglet N, Liu Y H, D. Sazou D, Findsen E, Faure D, Courieres T D & Kadish K M (1991) *Inorg Chem* 30, 1898-1905
26 Schenning A P H J, Feiters M C & Nolte R J M (1993) *Tetrahedron Lett* 34, 7077-7080
27 Neumann B (2001) *J Phys Chem B* 105, 8268-8274
28 Kano K, Minamizona H, Kitae T & Negi S (1997) *J Phys Chem A* 101, 6118-6124
29 Kano K, Fukuda K, Wakami H, Nishiyaku R & Pasternack R F (2000) *J Am Chem Soc* 122, 7494-7502
30 Dancil K P S, Hilario L F, Khoury R G, Mai K U, Nguyen C K, Weddle K S & Shachter A M (1997) *J Hetrocycl Chem* 34, 749-755
31 Gray G W & Jones B (1954) *J Chem Soc* 1467-1470
32 Takagi S, Yamamura T, Nakajima M, Ishiguro K, Kawanishi Y, Nihojima S, Tsuchiya H, Saito T & Sasaki Y (1981) *Bull Chem Soc Jpn* 54, 3879-3880
33 Fleischer F B & Hambright F (1970) *Inorg Chem* 9, 1799-1804
34 Huang C (1969) *Biochemistry* 8, 344-352
35 Awasthi A, Chaudhary S & Chauhan S M S, (1999) *Indian J Biochem Biophys* 36, 118-124
36 Jane Y S & Shih J S (1994) *J Chin Chem Soc* 41, 159-166
37 White W I in *The Porphyrins* (1978) (D. Dolphin, ed.), Vol. 5, pp. 303, Academic: New York
38 Wang L, Takahashi T, Ohno H & Tsuchida E (1989) *J Macromol Sci Chem* A 26, 481-489
39 Shelnutt J A, Dobry M M & Satteriee J D (1984) *J Phys Chem* 88, 4980-4987
40 Chang C K (1977) *J Hetrocycl Chem* 14, 1285-1288
41 Wasielewski M R, Niemczyk M P & Sveek, W A (1982) *Tetrahedron Lett* 23, 3215-3218
42 Chang C K (1979) *Adv Chem Ser* 173, 162-176
43 Kano K, Takei M & Hashimoto S (1990) *J Phys Chem* 94, 2181-2187
44 Gallagher W A & Elliot W B (1973) *Ann N Y Acad Sci* 206, 463-469
45 Pasternack R F, Bustamante C, Cllings P J, Giannetto A & Gibbs E J (1993) *J Am Chem Soc* 115, 5393-5399
46 Pasternack R F & Collins P J (1995) *Science* 269, 935-939
47 Nishide H, Mihagashi.K & Tsuchida E (1977) *Biochem Biophys Acta* 498, P208
48 Inamura I & Uchida K (1991) *Bull Chem Soc Jpn* 64, 2005-2007
49 Takami A & Mataga N (1987) *J Phys Chem* 91, 618-622